

Self-Steepening and Self-Compression of Ultrashort Optical Pulses in a Defocusing CdS Crystal

J.-F. Lami, S. Petit, and C. Hirlimann

Groupe d'Optique Non-Linéaire et d'Optoélectronique, Institut de Physique et Chimie des Matériaux de Strasbourg, Unité Mixte CNRS-ULP (UMR 7504), 23 rue du Loess, BP 20 CR, F67037 Strasbourg Cedex, France

(Received 25 September 1998)

Some consequences of the nonlinear propagation of a visible optical pulse in CdS, in a regime where the nonlinear index of refraction is negative, have been exhibited using a time-of-flight technique in the femtosecond regime. The self-steepening of the optical pulse is evidenced directly in the time domain. Self-shortening of the pulse occurs on a distance as short as $130\ \mu\text{m}$ opening the way of direct optical compression inside semiconductor lasers. Tunable optical soliton propagation is predicted which could be useful for multiplexing purposes. [S0031-9007(98)08328-8]

PACS numbers: 78.40.Fy, 42.65.Re, 42.65.Sf, 78.47.+p

Self-steepening [1–4] was first theoretically and experimentally studied by the end of the 1960s. Its effect on self-phase modulation (SPM) broadened spectra was first considered in liquids with large optical Kerr constants in the regime where light propagates in self-trapped filaments [5,6]. During the 1980s, self-steepening had been widely considered because of its importance during pulse propagation in optical fibers [7–9]. Except for a pioneering work in rubidium vapor [1], evidence of self-steepening was always obtained using indirect spectral measurements exhibiting an asymmetric broadening of the self-phase modulated spectrum of a propagating optical pulse. Such an analysis is ambiguous when, for example, the relaxation time of the medium where the propagation takes place is smaller than the pulse duration [5]. A masking of the self-steepening effect also shows up in the femtosecond regime, in optical fibers with a slow Raman response (≈ 60 fs) [2]. A short finite relaxation time always induces a steepening of the trailing edge of the temporal shape of a light pulse when the nonlinear refractive index is positive. In this work, we present what we believe is the first complete dynamical propagation study of a short optical pulse giving insight into both the intensity amplitude variation and the spectral behavior. We found two reasons to choose the II-VI semiconductor CdS as a propagation medium: (i) nowadays, its linear and nonlinear optical parameters are known with a good precision; (ii) experimental conditions can be chosen to steepen the leading edge of a propagating pulse.

Two series of experiments were performed: a degenerate pump-probe experiment used to measure the sign and amplitude of the nonlinear refractive index, already giving clues for self-steepening, and a time-of-flight experiment that allowed for the direct observation of self-steepening and self-compression of optical pulses. Both experiments were performed at room temperature. In these experiments we used as a sample bulk cadmium sulfide in the form of a high quality platelet, $130\ \mu\text{m}$ in thickness, vapor grown in an argon atmosphere, in a thermal furnace. During the growth process, the argon flux was kept be-

tween 0.3 and 3 l/min and the furnace maximum temperature was kept between 1050 and 1090 °C [10]. X-ray scattering measurements showed that the sample is in hexagonal wurtzite structure. The optical c axis lies in the plane of the platelet; its direction was determined through linear optical transmission measurement at the band gap energies [11]. Optical room temperature transmission measurement showed that the band gap of the sample was 2.48 eV, when the electric field of light is parallel to the c axis.

For the degenerate pump-probe experiment, optical pulses, 150 fs in duration, at 627-nm central wavelength, were generated using a dispersion compensated colliding pulse mode-locked dye laser oscillator [12]. These pulses were amplified [13] with a doubled Nd:YAG laser, at a 20-Hz repetition rate, up to an energy of $1\ \mu\text{J}$, allowing focused intensities up to $80\ \text{GW}/\text{cm}^2$. The pump beam was focused down to an e^{-2} radius of $36\ \mu\text{m}$. The probe pulses were kept down to intensities less than a few percent of the pump intensity and the pump was linearly cross polarized with the probe. Its polarization was set to be parallel to the c axis of the bulk CdS crystal in order not to induce any spurious birefringence. Scattered light from the pump was rejected by linearly analyzing the light coming out of the sample parallel to the probe polarization. The time coincidence between pump and probe, as well as the duration of the light pulses, was determined by replacing the sample with a $200\text{-}\mu\text{m}$ thick, phase matched, KDP (KH_2PO_4) crystal and recording an autocorrelation trace. At the exit of the amplifier a prism pair optical compressor was adjusted in order to compensate for the positive group velocity dispersion (GVD) induced by the various optical elements placed on the light path, so that the optical pulses were quasi-Fourier transform limited with $\Delta\nu\Delta t$, spectral width times duration relationship, equal to 0.48 (assuming a Gaussian shape).

The pump pulse induces in the crystal a nonlinear variation of the refractive index $n(\mathbf{r}, t)$ as a function of the spatial coordinates \mathbf{r} and the time t . The effects

of this variation on the probe pulse were measured by analyzing the transmitted light using a 25-cm focal length spectrograph and an optical multichannel analyzer. The frequency of the maximum of the probe spectrum was recorded as a function of the time delay between the pump and the probe after an automatic numerical average over five measurements, to improve the signal to noise ratio. The laser intensity fluctuations were estimated to be of the order of 10%. Figure 1 shows the experimental data obtained from this degenerate pump-probe experiment. The experimental curve is a clear phase modulation signature and exhibits two main features: the frequency of the maximum is up-shifted first; then the obtained curve is asymmetrical with a larger displacement toward the higher frequencies than toward the lower ones.

As the instantaneous frequency shift due to phase modulation varies as $\delta\omega \propto -n_2 \partial I(t)/\partial t$, to a first approximation, the apparition of blue components on the leading front of the pulse envelope immediately indicates that the nonlinear refractive index n_2 of the crystal is negative. Under our experimental conditions, the ratio of the photon energy to the band gap is 0.8 and it has been shown that for semiconductors, n_2 is negative when operating in the two-photon absorption (TPA) regime, with a photon energy to band gap ratio larger than 0.7. In this regime, the TPA and the quadratic Stark effect are the main contributors to the nonlinear refractive index [14] and solitonlike pulse propagation has been reported [15], but self-compression has never been observed.

Because this experiment has been performed in a wavelength degeneracy of the pump and the probe, walkoff between them cannot be invoked to explain the observed frequency asymmetry. Self-steepening of the

leading edge of the pulse time envelope is the simplest mechanism which can be thought of to account for it. Modeling of the experiment therefore implies to add a self-steepening term to the nonlinear wave equation [16]. Our experiment of two copropagating pulses in a nonlinear crystal is then well described by the following coupled differential equations:

$$\frac{\partial A_x}{\partial z} + \frac{1}{v_g} \frac{\partial A_x}{\partial t} + \frac{i}{2} k^{(2)} \frac{\partial^2 A_x}{\partial t^2} = \left(i \frac{\omega n_2}{c} - \frac{\beta_2}{2} \right) \frac{\epsilon_0 c}{2n_0} |A_x|^2 A_x - \frac{n_2 \epsilon_0}{n_0} |A_x|^2 \frac{\partial A_x}{\partial t}, \quad (1a)$$

$$\frac{\partial A_y}{\partial z} + \frac{1}{v_g} \frac{\partial A_y}{\partial t} + \frac{i}{2} k^{(2)} \frac{\partial^2 A_y}{\partial t^2} = i \frac{\omega n_2 \epsilon_0}{n_0} |A_x|^2 A_y. \quad (1b)$$

A is the complex amplitude of the electric field as a function of the spatial propagation parameter z and the time t , v_g is the group velocity of the light pulse, $k^{(2)} = 3.42 \text{ fs}^2/\mu\text{m}$ is the GVD parameter, n_0 and n_2 are, respectively, the linear and nonlinear refractive indexes of the crystal, ϵ_0 is the permittivity of the vacuum, c is the light speed in vacuum, ω is the central pulsation of the optical pulses, and $\beta_2 = 2.7 \text{ cm/GW}$ [17] is the TPA coefficient. Equation (1a), respectively, Eq. (1b), refers to the propagation along the z axis of the pump, respectively, the probe, pulse which is polarized along the x axis, respectively, the y axis. Because of the thinness of the sample, the defocusing of the beam is negligible. The theoretical model found in Ref. [18] predicts an increase of the radial extension of the beam diameter of less than 0.05% in our sample. Therefore both nonlinear wave equations (1) have been integrated along the radial spatial coordinate r . The linear absorption is also negligible since the photon energy is about 500 meV below the band gap energy. In addition to GVD, shown as the third term on the left-hand side of Eq. (1a), because of its high intensity, the pump pulse experiences SPM, described by the first term on the right-hand side of Eq. (1a), unsaturated [17] TPA, second term on the right-hand side of that same equation, and self-steepening shown as the last term of that first equation. According to Ref. [19], the stimulated Raman scattering can be neglected because the spectral broadening due to the phase modulation is much larger than the one due to the amplitude modulation. In comparison the weak probe pulse does experience only cross-phase modulation induced by the pump pulse in the medium [last term of Eq. (1b)]. The parameters used in Eq. (1) can be expressed in terms of familiar parameters [2]: the dispersion length L_D , the nonlinear length L_{NL} , and the self-steepening parameter s . In our experimental situation, $L_D = 3.2 \text{ mm}$, $L_{NL} = 16 \mu\text{m}$, and $s = 0.003$. The inset in Fig. 1 shows the spectrum of the probe pulse as a solution of Eq. (1) versus the time delay between the pump and probe pulses. The simulated curve exactly

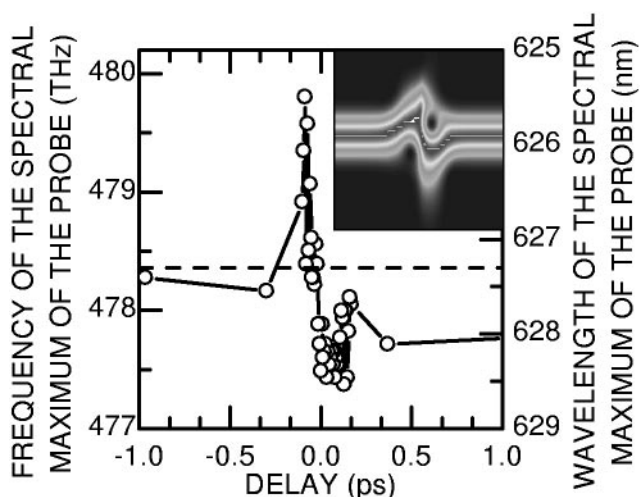


FIG. 1. Frequency shift of the spectral maximum of the probe pulse versus time delay between pump and probe pulses. The solid line is a guide to the eyes. In the inset is shown the probe spectrum versus the time delay as a result of the simulation described in the text. The full extension of the scales is the same as for the main figure. The gray levels correspond to the different intensities of the spectrum.

reproduces the two main features of the experimental data: peak-to-valley shape and asymmetry. From this model, we can adjust the experimental curve and deduce a nonlinear refractive index of $-3 \times 10^{-13} \text{ cm}^2/\text{W}$ which is in good agreement with a value previously obtained with an interferometric measurement [20]. Equation (1a) also predicts a time compression of the pump pulse when traveling through the sample. The understanding of this effect is as follows. The negative nonlinear refractive index of the medium induces a spectral broadening of the pulse through SPM with the higher frequencies being generated before the lower ones. The regular positive dispersion of the group velocity, which implies high frequencies to travel slower than the low frequencies, resynchronizes all the new frequencies and yields a time compression of the optical pulse.

In order to present clear-cut evidence of self-steepening and self-compression, a time-of-flight experiment was performed to measure dynamical intensity reshaping of an ultrashort optical pulse traveling through the same 130- μm thick CdS crystal. The source of the optical pulses is quite similar to the one previously described, except for the pulse amplification that was performed with a doubled Nd:YLF laser at a 1-kHz repetition rate as an energy source for the light amplifier. This system produces 105-fs, 900-nJ optical pulses at 625 nm. A beam splitter separates the beam into two parts with energies of 630 and 270 nJ. The first pulse travels through a 9-mm-long, 4- μm core diameter optical fiber to generate a white light continuum, which is then compressed in a double-pass prism pair. The resulting pulse having a 45-fs duration is used as a reference pulse. The second pulse travels through an optical delay line and is focused down to an e^{-2} radius of 33 μm on the CdS crystal, with an energy of 80 nJ and a 105-fs duration. It acts as the propagating probe. The light transmitted through the crystal is collimated and focused down together with the reference pulse on a nonlinear 200- μm -thick phase-matched KDP crystal in a background-free cross-correlation geometry. By varying the time delay between the two pulses, a photomultiplier tube detecting the sum-frequency signal allows us to record intercorrelation traces of the nonlinearly propagating probe pulse.

Intercorrelation traces were recorded with and without the CdS sample on the way of the probe, and for high and low intensities of the probe pulse. They are shown on a normalized scale in Fig. 2. Since the duration of the reference pulse is at least 2 times shorter than the one of the probe, the intercorrelation traces are good representations of the temporal profile of the probe. The left part of Fig. 2 shows the original probe pulse envelope with a slight asymmetry on the trailing edge created inside the laser amplifier by the disappearance of the leading edge of the pulses in their crossing of the saturable absorbers. Except for the slight asymmetry, the intercorrelation trace measured without the crystal on the way (open triangles

in Fig. 2) is perfectly fitted by the intercorrelation formula of two Gaussian pulses having 45- and 105-fs time duration, respectively, in excellent agreement with durations deduced from separate autocorrelation measurements. On the right side of the figure are shown the low intensity correlation (0.2 GW/cm², linear propagation, open squares) and high intensity correlation (15 GW/cm², nonlinear propagation, open circles). Steepening of the leading edge and pulse compression are readily observable. The high intensity correlation trace is shifted toward early time delays by 21 fs. This shift is a direct consequence of an increase of the group velocity when the light intensity increases and n_2 is negative. This 21-fs delay corresponds to a 2% increase in the group velocity. In order to ease the observation of the pulse envelope reshaping, the inset in Fig. 2 shows numerical derivatives of the probe pulse correlations which underline both the steepening of the leading edge (peak-to-peak asymmetry increase) and the duration shortening (peak-to-peak time delay narrowing).

In Fig. 3 we report the normalized low (open squares) and high (open circles) intensity intercorrelations of the pulse after propagation through the sample. The time delay origins for both traces have been taken the same for the purpose of comparing their duration. The 105-fs incoming pulse experiences regular positive GVD along its propagation through the sample. This shows up as a broadening of the low intensity intercorrelation trace which, after deconvolution from the 45-fs duration of the reference pulse, corresponds to a 115-fs full width at half maximum duration of the probe. The high intensity

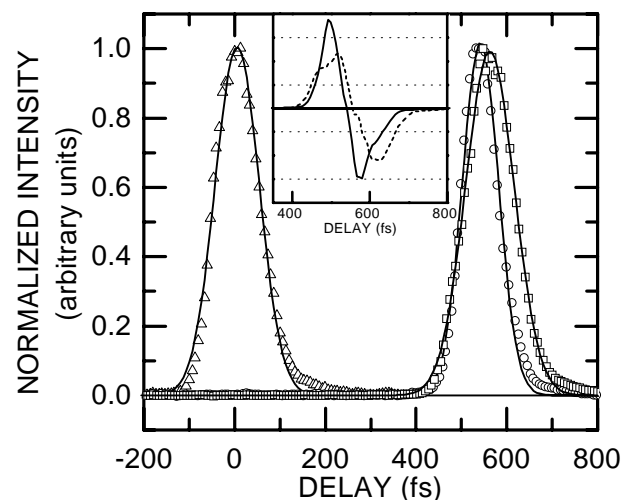


FIG. 2. Normalized time-of-flight measurements. Open triangles: 15-GW/cm² probe pulse in air. Open circles: 15-GW/cm² probe pulse propagating through a 130- μm -thick CdS sample. Open squares: 0.2-GW/cm² probe pulse through the sample. The main delay between traces is accounted for by group velocity delaying. The solid lines are fits obtained according to the procedure described in text. Inset: Intercorrelations numerical derivatives of the linearly propagating probe pulse (dashed line) and the nonlinearly propagating one (solid line).

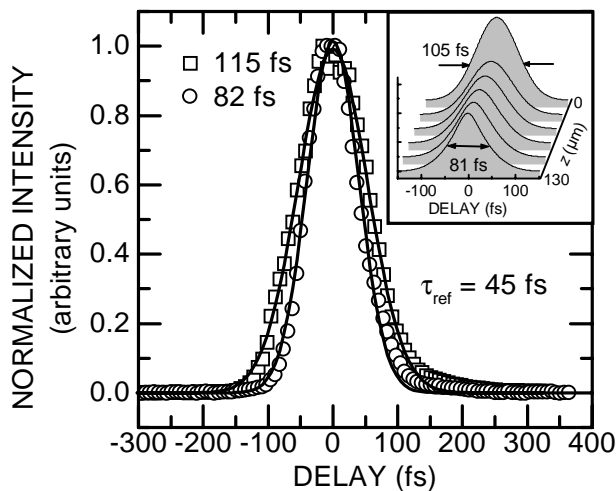


FIG. 3. Normalized intercorrelation traces of the reference and the transmitted probe pulses for 15-GW/cm^2 (open circles) and 0.2-GW/cm^2 (open squares) intensities. The two curves maxima have been superimposed. The inset shows the simulated temporal profile evolution of a 105-fs pulse propagating through a $130\text{-}\mu\text{m}$ -thick CdS crystal.

intercorrelation trace, on the contrary, exhibits a pulse duration shortening down to 82 fs. This 22% narrowing results from the balance between the negative dispersion of the new frequencies created through SPM and the regular positive GVD of the frequencies. As the spectral content of the pulse broadens along the propagation its duration decreases. Modeling of the self-compression effect has been performed again by numerically solving Eq. (1a) for Gaussian shaped pulses, and the result is shown in Fig. 3. It must be noted that no fitting is done; only the experimental values of the various parameters are injected in the model calculation. The agreement with the experiment is excellent as can be seen in the figure. The intensity decrease observed at the entrance of the sample ($z = 0$) is due to reflection. At least two possible applications of these findings can be envisioned.

Recent developments in the technology of semiconductor lasers [21,22], such as the introduction of semiconductor saturable absorbers, have led to the generation of ultrashort light pulses ($\Delta t \approx 500$ fs). Further progress toward generating even shorter pulses requires intracavity GVD compensation. Our results do show that this could be achieved by tailoring the band gap of the semiconductor inside the laser cavity in order to reach the self-steepening self-compression regime. Moreover, a new kind of soliton propagation can be predicted in which the sign of GVD and SPM are reversed as compared to the situation encountered by light pulses propagating in silica optical fibers. In the latter case the central wavelength of the soliton spectrum is univocally determined by the energy position of the residual OH bonds in the material. In semiconductors, on the contrary, the nonlinear refractive index is negative over 25% of the high energy side

of their band gap while GVD remains positive, opening the way to tunable solitons. Optical soliton data transfer and processing will probably highly benefit from this new frequency multiplexing opportunity.

A nonlinear refractive index of $-3 \times 10^{-13} \text{ cm}^2/\text{W}$ has been measured in a CdS crystal, using a spectrotemporal experiment performed with 150-fs lasting optical pulses at 2-eV photon energy. A time-of-flight experiment using an ultrashort reference pulse allowed the study of the intensity envelope reshaping experienced by an optical pulse nonlinearly propagating along $130 \mu\text{m}$ in the nonlinear medium. That way self-steepening and a 22% time self-compression of optical pulses have been evidenced.

- [1] D. Grischkowsky, E. Courtens, and J. A. Armstrong, *Phys. Rev. Lett.* **31**, 422 (1973).
- [2] G.P. Agrawal, in *Nonlinear Fiber Optics*, Optics and Photonics Series, edited by P.F. Liao, P.L. Kelley, and I. Kamirow (Academic Press, San Diego, 1995), 2nd ed., pp. 113–115.
- [3] D. Mestdagh and M. Haelterman, *Opt. Commun.* **61**, 291 (1987).
- [4] J.T. Manassah, in *The Supercontinuum Laser Source*, edited by R.R. Alfano (Springer-Verlag, New York, 1989), p. 184.
- [5] T.K. Gustafson, J.P. Taran, H.A. Haus, J.R. Lifshitz, and P.L. Kelley, *Phys. Rev.* **177**, 306 (1969).
- [6] R.J. Joenk and R. Landauer, *Phys. Lett.* **24A**, 228 (1967).
- [7] N. Tzoar and M. Jain, *Phys. Rev. A* **23**, 1266 (1981).
- [8] D. Anderson and M. Lisak, *Phys. Rev. A* **27**, 1393 (1983).
- [9] E. Bourkoff, W. Zhao, and R.I. Joseph, *Opt. Lett.* **12**, 272 (1987).
- [10] J.-I. Chikawa and T. Nakayama, *J. Appl. Phys.* **35**, 2493 (1964).
- [11] M. Balkanski and J. des Cloizeaux, *J. Phys. Radium* **21**, 825 (1960).
- [12] J.A. Valdmanis, R.L. Fork, and J.P. Gordon, *Opt. Lett.* **10**, 131 (1985).
- [13] P.C. Becker, A.G. Prosser, T. Jedju, J.D. Kafka, and T. Baer, *Opt. Lett.* **16**, 1847 (1991).
- [14] M. Sheik-Bahae *et al.*, *IEEE J. Quantum Electron.* **27**, 1296 (1991).
- [15] P. Dumais, A. Villeneuve, and J.S. Aitchison, *Opt. Lett.* **21**, 260 (1996).
- [16] G.P. Agrawal, P.L. Baldeck, and R.R. Alfano, *Phys. Rev. A* **40**, 5063 (1989).
- [17] J.-F. Lami, P. Gilliot, and C. Hirlimann, *Phys. Rev. Lett.* **77**, 1632 (1996).
- [18] B. Gross and J.T. Manassah, *Opt. Commun.* **126**, 269 (1996).
- [19] Y. Guozhen and Y.R. Shen, *Opt. Lett.* **9**, 510 (1984).
- [20] C. Hirlimann, E. Wassmuth, E. Kling, S. Petit, and M. Pereira dos Santos, *Appl. Phys. Lett.* **65**, 959 (1994).
- [21] A.G. Deryagin *et al.*, *Electron. Lett.* **30**, 309 (1994).
- [22] S. Arahira, Y. Matsui, and Y. Ogawa, *IEEE J. Quantum Electron.* **32**, 1211 (1996).